






Article

Osteogenic Differentiation Modulates the Cytokine, Chemokine, and Growth Factor Profile of ASCs and SHED

Federico Mussano ^{1,*},[†] , Tullio Genova ^{1,2},[†] , Sara Petrillo ³, Ilaria Roato ⁴ ,
Riccardo Ferracini ⁵ and Luca Munaron ²

¹ CIR Dental School, Department of Surgical Sciences UNITO, via Nizza 230, 10126 Turin, Italy; tullio.genova@unito.it

² Department of Life Sciences and Systems Biology, UNITO, via Accademia Albertina 13, 10123 Turin, Italy; luca.munaron@unito.it

³ Department of Molecular Biotechnology and Health Sciences, UNITO, Via Nizza 52, 10126 Turin, Italy; sara.petrillo@unito.it

⁴ Center for Research and Medical Studies, A.O.U. Città della Salute e della Scienza, 10126 Turin, Italy; roato78@libero.it

⁵ Department of Surgical Sciences (DISC), Orthopaedic Clinic-IRCCS A.O.U. San Martino, 16132 Genoa, Italy; riccardoferraciniweb@gmail.com

* Correspondence: federico.mussano@unito.it; Tel.: +39-011-091-8360

† These authors contributed equally to this work.

Received: 16 April 2018; Accepted: 11 May 2018; Published: 14 May 2018



Abstract: Great efforts have been made to improve bone regeneration techniques owing to a growing variety of sources of stem cells suitable for autologous transplants. Specifically, adipose-derived stem cells (ASCs) and stem cells from human exfoliated deciduous teeth (SHED) hold great potential for bone tissue engineering and cell therapy. After a preliminary characterization of the main biomolecules ASCs and SHED released in their conditioned media, cells were kept both in normal and osteo-inducing conditions. Conventional assays were performed to prove their osteogenic potential such as quantitative real-time polymerase chain reaction (qRT-PCR) (for RUNX-2, collagen type I, osteopontin and osteonectin), alkaline phosphatase activity, osteocalcin production, and von Kossa staining. Conditioned media were tested again after the osteogenic induction and compared to maintaining condition both at base line and after 14 days of culture. The osteogenic condition inhibited the release of all the biomolecules, with the exception, concerning SHED, of growth-regulated alpha protein precursor (GRO α), and, to a lesser extent, interleukin (IL)-8. In conclusion, our data support that undifferentiated ASCs and SHED may be preferable to committed ones for general cell therapy approaches, due to their higher paracrine activity. Osteoinduction significantly affects the cytokine, chemokine, and growth factor profile in a differential way, as SHED kept a more pronounced pro-angiogenic signature than ASCs.

Keywords: mesenchymal stem cells (MSCs); adipose-derived stem cells (ASCs); stem cells from human exfoliated deciduous teeth (SHED); Bio-Plex

1. Introduction

With more than 2 million bone grafts performed annually worldwide, bone reconstruction is a primary task of regenerative medicine [1]. Autologous bone graft is deemed the safest and most effective grafting procedure [2]. However, the autograft entails a surgical “donor” site, which often brings additional morbidity, including pain and infections [3]. Moreover, the bone source is usually

limited [4]. Xenografts, coming from other species, are hindered by the absence of cells and the possible contamination. Similarly, most available synthetic bone substitutes lack the ability to induce bone formation [5].

Whatever the type of grafting, the real challenge in bone tissue engineering is represented by critical-sized bone defect, meaning osseous injuries unable to heal spontaneously [6]. Only through an integrated approach will multidisciplinary teams succeed in fabricating complex scaffolds, including live cell populations endowed with the most sophisticated features of biomimicry [7], to set up a complex 3D tissue under the guidance of suitable biomolecular cues. To this end, the ideal stem cell should be abundant, accessible (i.e., harvested with a minimally invasive procedure), and capable of differentiating along multiple cell lineages in a reproducible manner [7,8].

Human mesenchymal stem cells (MSCs) have been shown to be particularly suitable for auto-transplant procedures. Apart from bone marrow [9], MSCs can be obtained from umbilical cord [10], adipose tissue [11], placenta [12,13], human synovial membrane [14], and dental pulp of deciduous teeth [15]. Teeth and the surrounding tissues are indeed an important source of MSCs. They can be categorized according to their origin in dental pulp stem cells (DPSCs), periodontal ligament stem cells, stem cells from apical pulp, dental follicular precursor cells, and stem cells from human exfoliated deciduous teeth (SHED) [16].

In the present study, the authors decided to focus on two easily attainable cell types, adipose-derived stem cells (ASCs) and SHED, as the most promising sources of MSCs in the dental field. Described for the first time in 2001 [17], ASCs, thus named as per the consensus of the International Fat Applied Technology Society [18], represent a plastic-adherent, multi-potent cell population that can be collected in large quantities with low possibility of donor site morbidity, during liposuction procedure [19]. SHED are highly proliferative, clonogenic cells capable of differentiating into a variety of cell types, including cell-mediating bone formation in vivo [20,21]. Owing to their short period of availability, limited to the primary dentition, SHED have been considered a prototypical source for banking [22].

The use of MSCs is mandatory for any bone engineering approach [23,24]. Besides their actual role in building new tissue, these cells are also attracting growing interest as “vehicles” for paracrine signals, in what is usually defined as cell therapy. Surprisingly, however, sporadic data are available thereof [25] and only minor information has been published comparing different mesenchymal cell types [26]. To the authors’ knowledge, indeed, no comparative studies have assessed the biomolecular profile characterizing ASCs and SHED so far, nor was the osteogenic capacity of ASCs and SHED ever tested under this perspective. Hence, the aim of the present study was to compare the cytokine, chemokine, and growth factor profile of osteoinduced ASCs and SHED to possibly unveil advantages and pitfalls of adopting either cell type in the context of regenerative medicine.

2. Results

2.1. ASCs and SHED Displayed Different Cell Morphology and Biomolecular Profiles at First Passage

At the first in vitro cell culture passage after harvesting, ASCs appeared more spread out (Figure 1A), while SHED presented a higher nucleus to cytoplasm ratio (Figure 1B). ASCs and SHED showed a comparable phenotype consistent with that of MSCs [27]. Both cell types expressed the main mesenchymal markers CD105, CD44, CD73, and CD90 and were negative for CD45. No significant difference in the percentage expression of these markers was found in the two populations (Figure 1C,D).

To assess the expression profile of growth factors, cytokines, and interleukins produced by these MSCs, a standard panel of factors was evaluated (Figure 2, Table 1). They include various anti- and pro-inflammatory interleukins (ILs), such as IL-6, -8, -10, and -12, as well as growth and angiogenic factors like growth-regulated alpha protein precursor (GRO α) and vascular endothelial growth factor (VEGF), which were all significantly more abundant in ASCs than in SHED. On the

contrary, while the levels of β -nerve growth factor (β -NGF), stem cell factor (SCF), and stromal cell-derived factor-1 α (SDF-1 α) were hardly detectable in ASCs, their production was significant in SHED, even in conspicuous quantities in the case of SDF-1 α . Similarly, SHED released more monocyte chemotactic protein 1 (MCP-1) and hepatocyte growth factor (HGF) (ten times higher levels) than ASCs. Macrophage migrator Inhibitory Factor (MIF) was well represented in both cell populations.

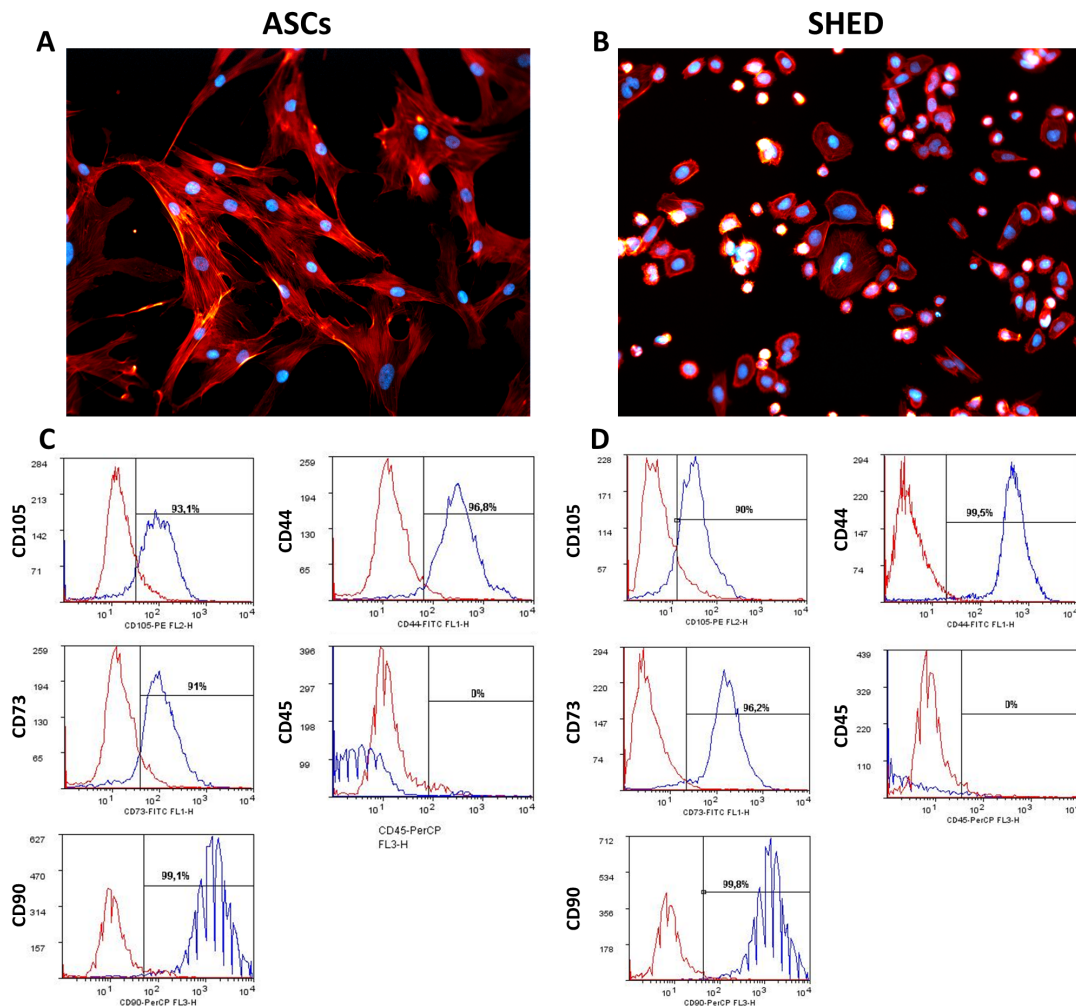


Figure 1. Cell morphology of adipose-derived stem cells (ASCs) (A) and stem cells from human exfoliated deciduous teeth (SHED) (B), phalloidin staining (in red) and DAPI (in blue) to mark respectively cytoskeleton and nuclei, magnification 400 \times . Cytofluorimetric characterization was obtained through CD105, CD44, CD73, CD90, and CD45 for ASCs (C), and SHED (D).

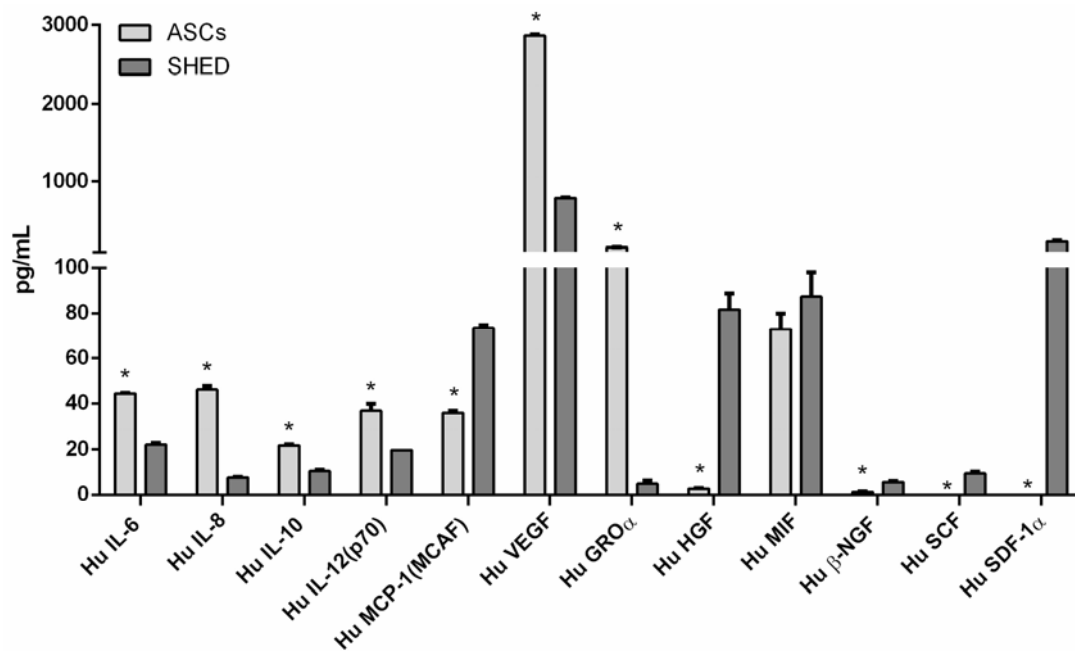


Figure 2. Bio-Plex quantification of factors produced by ASC and SHED at baseline. The evaluated factors are: interleukin-6 (IL-6), interleukin-8 (IL-8), interleukin-10 (IL-10), interleukin-12 (IL-12), monocyte chemoattractant protein-1 (MCP-1), vascular endothelial growth factor (VEGF), growth-regulated α protein precursor (GRO α), hepatocyte growth factor (HGF), macrophage migration inhibitory factor (MIF), β -nerve growth factor (β -NGF), stem cell factor (SCF), and stromal cell-derived factor 1- α (SDF-1 α). The symbol (*) indicates a significant difference between the two stem cells populations, considering a p -value < 0.05.

Table 1. Bio-Plex quantification of factors produced by ASC and SHED at baseline. The evaluated factors are expressed in pg/mL and are: interleukin-6 (IL-6), interleukin-8 (IL-8), interleukin-10 (IL-10), interleukin-12 (IL-12), monocyte chemoattractant protein-1 (MCP-1), vascular endothelial growth factor (VEGF), growth-regulated alpha protein precursor (GRO α), hepatocyte growth factor (HGF), macrophage migration inhibitory factor (MIF), β -nerve growth factor (β -NGF), stem cell factor (SCF), and stromal cell-derived factor 1- α (SDF-1 α). *Italic fonts of numbers indicate a significant difference between the two stem cell populations, considering a p -value < 0.05.*

Biomolecule	Baseline	
	ASCs	SHED
Hu IL-6	44.40	22.12
Hu IL-8	46.13	7.76
Hu IL-10	21.78	10.55
Hu IL-12	36.76	19.72
Hu MCP-1	35.82	73.40
Hu VEGF	2867.41	786.37
Hu GRO α	161.90	4.90
Hu HGF	2.78	81.67
Hu MIF	72.90	87.28
Hu β -NGF	1.33	5.68
Hu SCF	0.01	9.51
Hu SDF-1 α	0.01	233.43

2.2. Cell Viability

The growth of ASCs and SHED was estimated under maintenance (growth medium, GM) and osteogenic (osteogenic medium, OM) conditions at day 1, 3, and 7 (Figure 3). Starting from day 1, the

proliferation rate was prevented in both ASCs and SHED grown in OM compared to GM. This trend became statistically significant at days 3 and 7 (Figure 3).

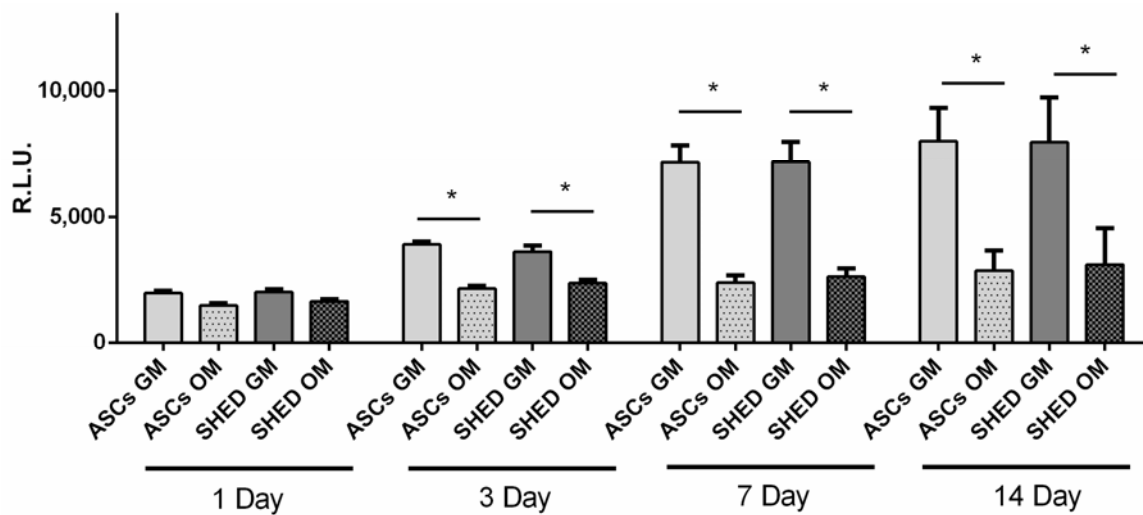


Figure 3. Cell viability assay. The assay was performed on ASCs and SHED cultured in growth medium (GM) or osteogenic medium (OM). Evaluations were made at 1, 3, 7, and 14 days from the beginning of the differentiation using CellTiter-Glo[®] luminescent assay. Cell number is expressed as relative luminescence units (RLU). The symbol (*) indicates a significant difference between basal condition (GM) and osteogenic media (OM) considering a *p*-value < 0.05.

2.3. Early Osteogenic Differentiation of ASCs and SHED

To assess the early osteogenic differentiation of ASCs and SHED, the transcript levels of RUNX-2 (Figure 4A) and collagen type I (Figure 4B) genes were evaluated through quantitative RT-PCR at days 3, 7, and 14. As a complementary assay to monitor the post-transcriptional level, alkaline phosphatase activity was also tested at day 7 (Figure 4C). These forms of evidence supported that both ASCs and SHED underwent proper osteogenic commitment, the bone markers being constantly higher in osteodifferentiated cells compared to the control (Figure 4). The statistical significance was achieved at day 7 in every assay.

2.4. Late Osteogenic Differentiation of ASCs and SHED

Late osteogenic differentiation of ASCs and SHED was evaluated by quantifying the transcriptional levels of osteopontin (Figure 5A) and osteonectin (Figure 5B) genes, which resulted in more expressed in OM condition at both day 7 and 14. Likewise, a significant enhancement of released osteocalcin was observed in osteoinduced cells compared to the controls at day 21 (Figure 5C). All these data clearly showed that ASCs and SHED were properly osteodifferentiated. As a further confirmation, the presence of calcified matrix was proven by von Kossa staining in osteoinduced ASCs and SHED at 21 days (respectively Figure 5D,E).

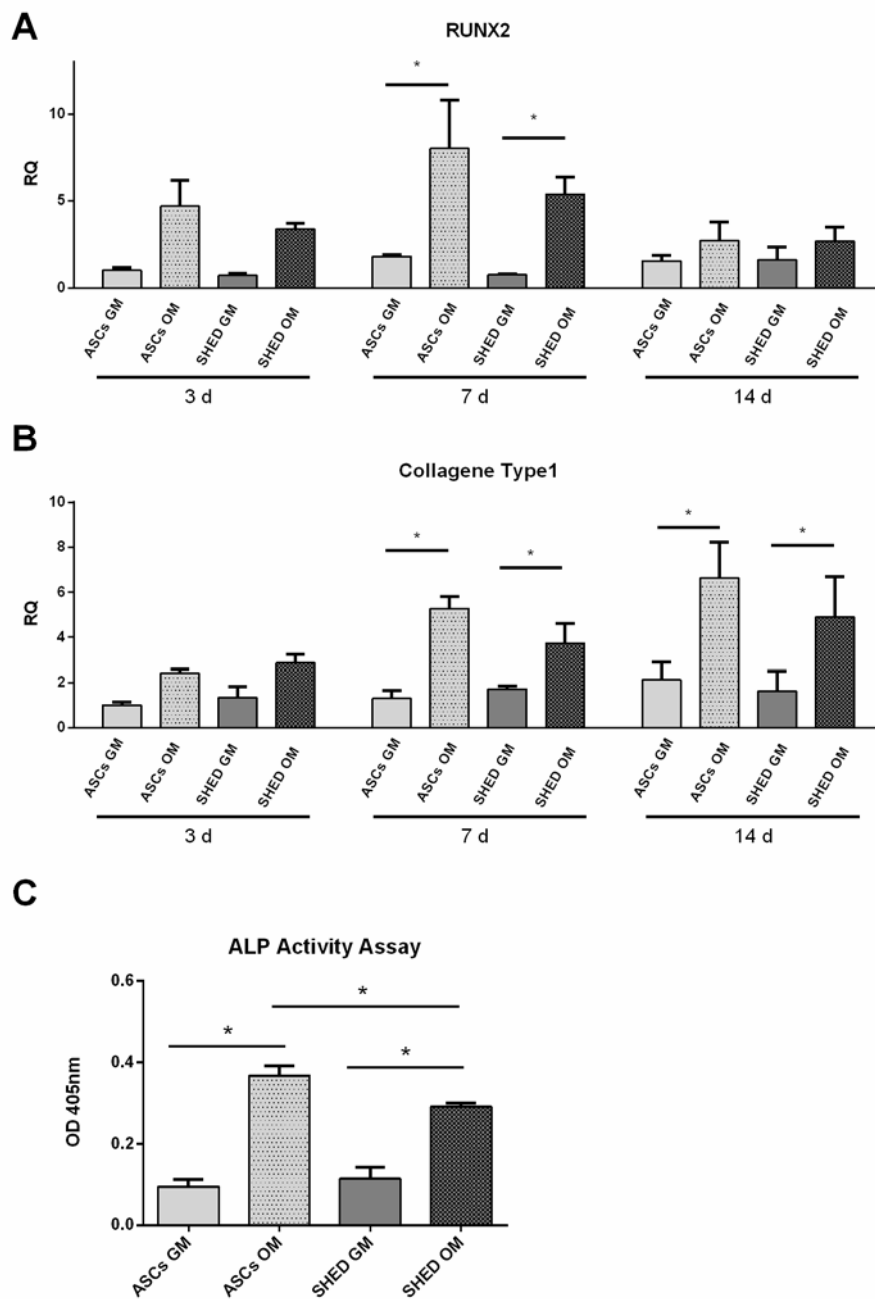


Figure 4. Early osteogenesis assessment based on quantitative real-time polymerase chain reaction (qRT-PCR) and alkaline phosphatase (ALP) activity assay. qRT-PCR analysis of osteogenic markers: RUNX2 (A), collagen type I (B), and ALP activity assay (C) performed on ASCs and SHED under basal conditions (GM) and in differentiating medium (OM). The symbol (*) indicates a significant difference between GM and OM condition considering a p -value < 0.05 , d: day.

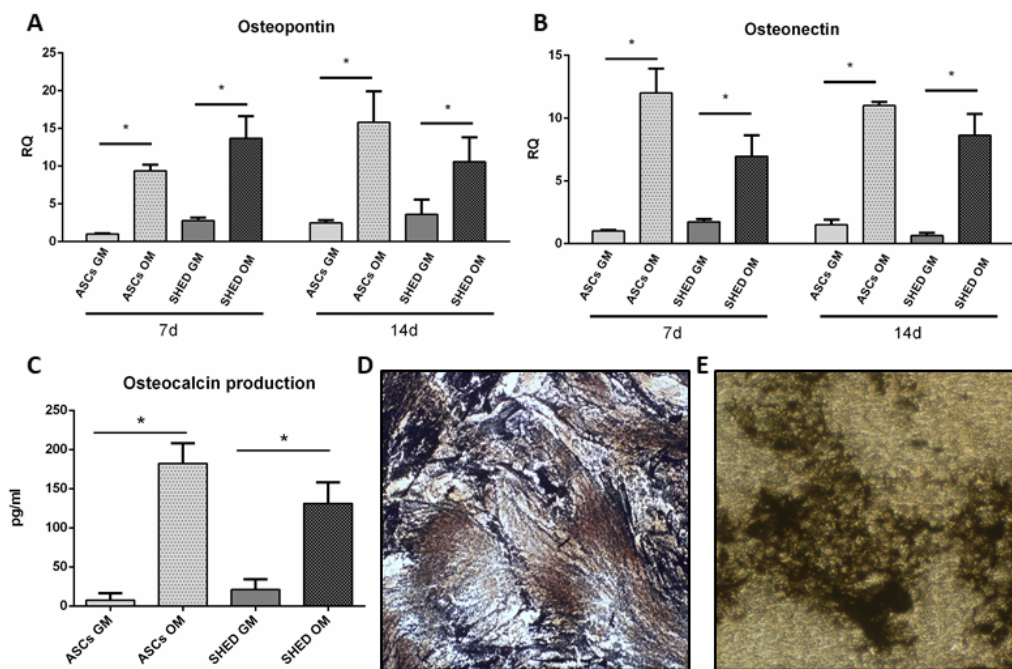


Figure 5. Late osteogenesis assessment based on qRT-PCR, ELISA detection of osteocalcin, and von Kossa staining. qRT-PCR analysis of osteopontin (A) and osteonectin (B) genes performed on ASCs (gray bar) and SHED (dark grey bar) under basal conditions (GM) and in osteo-differentiating medium (OM), d: day. Osteocalcin detection within conditioned media performed through ELISA (C). The symbol (*) indicates a significant difference between GM and OM condition considering a p -value < 0.05 . Von Kossa Staining of osteodifferentiated ASCs (D) and SHED (E) at day 21, magnification 100 \times .

2.5. The Biomolecular Profile of ASCs and SHED Was Modulated upon Culture in OM

The expression profile of growth factors, cytokines, and interleukins produced by ASCs and SHED was again detected with the same panel that was evaluated after the harvest (Figure 2). After 14 days of culturing in GM (Figure 6A,B, Table 2), ASCs increased their levels of IL-6, IL-8, and MCP, while SHED released more IL-6, IL-8, GRO α , MIF, and SDF1 α . The comparison of the cells conditioned in OM for 14 days (Figure 6C,D, Table 2) with the baseline of freshly harvested cells revealed that the osteogenic condition inhibits the release of all the biomolecules expressed by ASCs and SHED, with the exception for the latter of GRO α , and, to a lesser extent, IL-8.

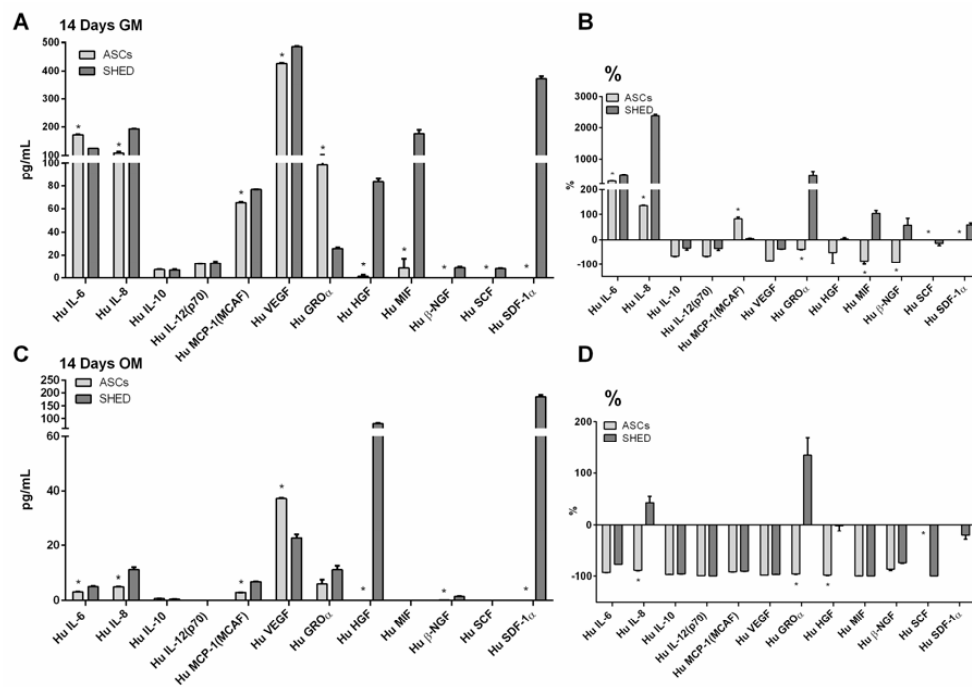


Figure 6. Bio-Plex quantification of factors produced by ASCs and SHED after 14 days of culturing in GM (A) and upon osteoinduction in OM (C). Side graphs comparing the relative variation of A and C (percentage) to the baseline after harvesting are shown respectively in (B) and (D) under the label %. The evaluated factors are: interleukin-6 (IL-6), interleukin-8 (IL-8), interleukin-10 (IL-10), interleukin-12 (IL-12), monocyte chemoattractant protein-1 (MCP-1), vascular endothelial growth factor (VEGF), growth-regulated alpha protein precursor (GRO α), hepatocyte growth factor (HGF), macrophage migration inhibitory factor (MIF), β -nerve growth factor (β -NGF), stem cell factor (SCF), and stromal cell-derived factor 1- α (SDF-1 α). All of the factors were analyzed in both populations, but b-NGF, SCF, and SDF-1 α were not expressed in ASC. The symbol (*) indicates a significant difference between the two stem cell populations, considering a p -value < 0.05.

Table 2. Bio-Plex quantification of factors produced by ASCs and SHED after 14 days of culturing in GM and upon osteoinduction in OM. The evaluated factors are expressed in pg/mL and are: interleukin-6 (IL-6), interleukin-8 (IL-8), interleukin-10 (IL-10), interleukin-12 (IL-12), monocyte chemoattractant protein-1 (MCP-1), vascular endothelial growth factor (VEGF), growth-regulated alpha protein precursor (GRO α), hepatocyte growth factor (HGF), macrophage migration inhibitory factor (MIF), β -nerve growth factor (β -NGF), stem cell factor (SCF), and stromal cell-derived factor 1- α (SDF-1 α). *Italic fonts of numbers indicate a significant difference between the two stem cell populations, considering a p -value < 0.05.*

Biomolecule	14 Days GM		14 Days OM	
	ASCs	SHED	ASCs	SHED
Hu IL-6	173.07	125.29	3.02	5.04
Hu IL-8	108.70	192.72	4.95	11.10
Hu IL-10	7.24	6.95	0.62	0.39
Hu IL-12	12.41	12.73	0.01	0.01
Hu MCP-1	65.23	76.71	2.87	6.80
Hu VEGF	426.58	486.12	37.25	22.67
Hu GRO α	98.51	25.85	5.99	11.03
Hu HGF	1.43	83.51	0.10	79.66
Hu MIF	8.54	176.84	0.10	0.00
Hu β -NGF	0.10	8.87	0.17	1.45
Hu SCF	0.01	8.02	0.01	0.10
Hu SDF-1 α	0.01	373.04	0.01	183.91

3. Discussion

In recent years, great efforts have been made to improve bone regeneration techniques, owing not only to the technological innovations in the field of material science, but also to a growing variety of sources of stem cells for autologous transplants [8,28]. Among all the possible options, MSCs hold great potential for bone tissue engineering [29]. In the present work, we focused our attention on ASCs and SHED [17,20,21,30] respectively due to their abundance and their accepted bankability based on cryopreservation [31]. Interestingly, we showed that ASCs and SHED display distinctive morphologies when they adhere on plastic culture dishes, as it was portrayed even here (Figure 1A,B) through immunofluorescent staining. The standard panel of markers used [27] qualified both cell types as mesenchymal stem cells (Figure 1C,D).

Despite their common mesenchymal nature, ASCs and SHED derive from different tissues, and the microenvironment in which these MSCs live may deeply affect their gene expression profile [32] as well as their secretome. Thus, the purpose of this study was to evaluate and compare the effect of osteodifferentiation on the biomolecular expression profile of ASCs and SHED. To accomplish this task, a standard panel of growth factors, cytokines, and interleukins was evaluated (Figure 2), through Bio-Plex assay [25]. This technique has multiple advantages over common ELISA kits, since it permits a large number of molecules to be analyzed in the same sample and also allows reproducible and comparable titration curves to be established [33,34].

We found that ASCs and SHED strongly differed in their basal expression of several biomolecules. Important factors like HGF and SDF-1 α were abundant in SHED but barely detectable in ASCs. Cloned as a mitogenic protein for hepatocytes [35], HGF promotes morphogenesis and cell survival. HGF was also proven to induce epithelial tubulogenesis/morphogenesis [36] and it has become a promising candidate for treating patients with impaired tissue function [37]. As for SDF-1 α , it is a strong chemoattractant for stem cells that has received growing attention as a means to recruit endogenous progenitor cells possibly leading to regeneration in situ [38]. SCF, the ligand of the tyrosine kinase receptor c-KIT, and β -NGF were more expressed by SHED than ASCs, but did not reach high levels. These biomolecules might sustain trophic mechanisms and cooperate to allow for the successful use of MSCs for musculoskeletal applications [39]. The pro-inflammatory cytokine MIF was almost equally produced in both cell types. ASCs released higher levels of multifunctional interleukins (IL-6, IL-8, IL-10, IL-12) and VEGF, the prototypical pro-angiogenic factor, than SHED, whilst GRO α was scarce in SHED, but fairly represented in ASCs.

Surprisingly, very little information is available in the literature concerning secretome of ASCs and SHED; indeed, it is quite rare to find reports where more than five cytokines/growth factors are analyzed at the same time. Different works reported the release of high amounts of VEGF by ASCs [40–42], similar to our result. Park et al. [43] examined the ASC secretion profile and its potential usage in treating skin ageing. Moreover, through the usage of enzyme-linked immunosorbent assay kits, these authors quantified HGF, which, in discord with our observation, resulted in the range of 670 pg/mL. The conspicuous production of HGF in SHED was instead described by Yamaguchi S et al. as was the low amount released by ASCs used in comparison [26], results which are pretty consistently in line with the outcome of our study (Figure 2).

Osteogenic condition inhibited cell proliferation, as it could be easily predicted, in accordance with previous literature [44,45]. Likewise, the efficacy of the osteo-inductive condition adopted was assessed with standard methods, which consistently confirmed that the in vitro differentiation sought occurred properly. Interestingly, we found that ASCs increased their levels of IL-6, IL-8, and MCP, while SHED augmented the release of IL-6, IL-8, GRO α , MIF, and SDF1 α when cells became confluent, as it was clearly portrayed in the Bio-Plex analysis at 14 days (Figure 6A).

The secretion of paracrine factors has been pointed out as a major way to enhance the healing process in numerous approaches based on ASCs [46,47] and SHED [48,49]. Based on these forms of evidence, the effect elicited by osteoinduction on the biomolecular profile of ASCs and SHED becomes of great interest. Osteogenic commitment tended to considerably downregulate the paracrine activity

and thus the release of notably useful factors when compared to the baseline condition (shortly after cell harvest). Quite relevantly, all the biomolecules decreased, with the only exception of GRO α and IL-8 in osteoinduced SHED. GRO α , also known as CXCL1, was described among the key angiogenic chemokines [50], while the pro-angiogenic role of IL-8 has been acknowledged since the paramount study by Koch and colleagues [51]. Owing to this pro-angiogenic cue, committed SHED could prove useful to implement *ex vivo* bone regenerative Good Manufacturing Practice compliant protocols, especially in the dental field.

4. Materials and Methods

4.1. Primary Cell Harvest and Culture

The primary human cells used in this study, adipose-derived stem cells (ASCs) and stem cells from human exfoliated deciduous teeth (SHED), were obtained from human volunteers between 1 January and 30 June 2013. The research was conducted following the protocols approved (in October 2012) by the Ethics Committee of the Clinica Fornaca di Sessant (usage of lipoaspiration product, protocol number EC20121008) and the CIR-Dental School of the University of Turin (harvest of deciduous teeth, protocol number CIR20121022). Written informed consent was always obtained from donors. As previously reported [17], ASCs were isolated and expanded from the lipoaspirates of ten different donors (mean age 25.6 ± 4.5 years, male/female = 5/5) at the Clinica Fornaca di Sessant, Turin. Following Miura's protocol [20], SHED were extracted from integer exfoliated deciduous teeth that were collected from ten children (9.2 ± 2.2 years) undergoing tooth extraction at the CIR-Dental School. For both cell types, the non-adherent cell populations were removed after 48 h and the adherent cell layer was washed twice with fresh medium. ASCs and SHED were maintained in growth medium (GM) consisting of RPMI (EuroClone S.p.A., Milan, Italy) enriched with sodium pyruvate and supplemented with 10% fetal bovine serum (Gibco BRL, Milan, Italy), penicillin-streptomycin 1:100, at 37 °C in humidified atmosphere with 5% CO₂. Cells were then continuously cultured following their harvest until fourth passage. To induce osteogenic differentiation, cells were cultured in "osteogenic medium" (OM) by supplementing GM with 10 mM β -glycerophosphate, 50 μ g/mL ascorbic acid, and 0.02 mg/mL dexamethasone [52,53].

4.2. Cell Morphology

As described elsewhere [54–56], cells were seeded at a concentration of 5×10^3 cells/well in a 24-well plate for 1 day. After fixing in 4% paraformaldehyde in phosphate buffered saline (PBS), cells were stained with rhodamine phalloidin and DAPI (Life Technologies, Milan, Italy) to mark actin network and nuclei, respectively. Images were acquired with a Nikon Eclipse Ti-E microscope using different a Nikon Plan 20X/0,10 (Nikon Instruments, Amsterdam, The Netherlands).

4.3. Phenotype of ASCs and SHED

Cell surface markers of ASCs and SHED were analyzed by flow cytometry. In detail, cells were identified as CD105, CD44, CD73, and CD90 positive cells and negative for CD45 expression. Standard labelling protocol was performed with the following antibodies fluorochrome-conjugated and isotypic controls: human CD105 PE (Invitrogen, Camarillo, CA, USA), CD73 FITC (kindly provided by Prof. Malavasi, University of Turin), CD44 FITC, CD45 PerCP, IgG1 PE and IgG2a PerCP (Miltenyi Biotech, Bergisch Gladbach, Germany), and IgG1 FITC-conjugated (Immunostep). As further control, unstained cells were also examined. About 10^5 events/sample were used for capture with CellQuest software. Data were analyzed with FlowLogic software (Miltenyi Biotech).

4.4. Detection of Interleukins, Chemokines, and Growth Factors by Bio-Plex System

To quantify a panel of major signaling molecules released within their medium, ASCs and SHED were kept in GM for 3 days until confluence to assess the baseline. Cells were also kept either in GM or

in osteodifferentiating medium for 14 days. The conditioned media thus produced by ASC and SHED after 2 hour starvation in RPMI were analyzed with the flexible Bio-Plex system (Bio-Rad Laboratories, Hercules, CA, USA), following the manufacturer's protocol, as described elsewhere [57,58]. At least two independent experiments were made per sample. The concentrations of the following specific biomolecules was measured: IL-6, IL-8, IL-10, IL-12, MCP-1, VEGF, GRO α , HGF, MIF, β -NGF, SCF, and SDF-1 α . Concentrations of the analytes are expressed in pg/mL.

4.5. Viability Assay

ASCs and SHED were plated at a density of 500 cells/well in 96-well culture dishes and the viability was assessed by CellTiter-Glo[®] (Promega, Milan, Italy) according to the manufacturer's protocol at 1, 3, 7, and 14 days [59,60]. The CellTiter-Glo[®] Luminescent Cell Viability Assay is a homogeneous method of determining the number of viable cells in culture based on quantitation of ATP as a marker of metabolically active cells. The amount of ATP is directly proportional to the number of viable cells in culture; for this reason, this assay can be used as an indicator of cell proliferation (as reported by manufacturer).

4.6. RNA Extraction and Real-time PCR Analysis

Total RNA was extracted using PureLink RNA Mini Kit (Ambion, Life Technologies Italy, Milan, Italy). For quantitative real-time polymerase chain reaction (qRT-PCR), 1 μ g total RNA was transcribed into complementary DNA by MultiScribe[®] Reverse Transcriptase (High-Capacity cDNA Reverse Transcription Kit, Thermo Fisher Scientific, Waltham, MA, USA) and PCR analysis was then assessed using TaqMan probes from Roche. Transcript abundance, normalized to 18s mRNA expression, is expressed as a fold increase over a calibrator sample. qRT-PCR was performed on a 7900HT Fast Real-Time PCR System (Applied Biosystems, Life Technologies Italy, Milan, Italy). Specific primers and probes were designed using the Universal Probe Library—Assay Design Center—Roche Life Science software (www.lifescience.roche.com) [61,62].

4.7. Alkaline Phosphatase Activity

Alkaline phosphatase activity (ALP) was determined colorimetrically as previously reported [63] and assessed at day 7. Cells were lysed with 0.05% Triton X-100 and incubated with the reagent solution containing phosphatase substrate (Sigma-Aldrich, Milan, Italy) at 37 °C for 15 min. A calibration curve of p-nitrophenol standards was always used. Alkaline phosphatase values were determined (Optical Density 405 nm) and normalized to the whole protein content, which was determined (Optical Density 562 nm) with a BCA[™] Protein Assay (Thermo Fisher Scientific).

4.8. Osteocalcin Detection

Following the manufacturer's protocol, osteocalcin (OCN) was measured in GM and OM media by means of Osteocalcin Elisa kit (KAQ1381 Invitrogen Corporation, Waltham, MA, USA) at day 21.

4.9. Von Kossa Staining

ASCs and SHED were grown in six-plate wells until day 21 in OM. Cells were washed once with PBS, then they were fixed with 4% paraformaldehyde for 10 min at room temperature prior to being washed again with PBS. Calcium salts were stained after von Kossa (vK) as reported previously [64], while representative pictures were captured under light microscopy by an Olympus camera.

4.10. Statistical Analysis

Data were analyzed by the use of GraphPad Prism6 (GraphPad Software, Inc., La Jolla, CA, USA) and Microsoft Excel (Microsoft Corporation, Redmond, WA, USA). Each experiment was repeated at

least three times. Statistical analysis was performed by using the Mann-Whitney non-parametric *t*-test. A *p*-value of <0.05 was considered significant [65,66].

qRT-PCR data were analyzed with GraphPad Prism 6 (GraphPad Software, Inc., La Jolla, CA, USA) by performing ordinary two-way ANOVA with Sidak's multiple comparisons test for grouped analyses or Mann Whitney test for column analyses.

5. Conclusions

In summary, these data suggest that undifferentiated ASCs and SHED may be preferable to committed ones for general cell therapy approaches, due to their higher paracrine activity. Osteoinduction significantly affects the cytokine, chemokine, and growth factor profile in a differential way, as SHED, differently from ASCs, developed a marked pro-angiogenic signature.

Author Contributions: F.M., L.M., and T.G. conceived and designed the experiments; T.G. and F.M. performed the cell biology experiments; S.P. performed the qRT-PCR; I.R. performed the flow-cytometry experiments. F.M., T.G., and I.R. analyzed the data. F.M., R.F., and L.M. wrote the manuscript.

Acknowledgments: The research was funded with a grant of the University of Turin (F.M.), which covered the costs to publish in open access.

Conflicts of Interest: The authors declare no conflict of interest. The founding sponsors had no role in the design of the study; in the collection, analyses, or interpretation of data; in the writing of the manuscript, and in the decision to publish the results.

Abbreviations

MSCs	Mesenchymal stem cells
ASCs	Adipose-derived stem cells
SHED	Stem cells from human exfoliated deciduous teeth
DPSCs	Dental pulp stem cells
GM	Growth medium
OM	Osteogenic medium
VEGF	Vascular endothelial growth factor
FGFs	Fibroblast growth factors
IGF-1	Insulin growth factor 1
IL-6	Interleukin-6
IL-8	Interleukin-8
IL-10	Interleukin-10
IL-12	Interleukin-12
MCP-1	Monocyte chemoattractant protein-1
GRO α	Growth-regulated alpha protein precursor
HGF	Hepatocyte growth factor
MIF	Macrophage migration inhibitory factor
β -NGF	β -Nerve growth factor
SCF	Stem cell factor
SDF-1 α	Stromal cell-derived factor 1- α
qRT-PCR	Quantitative real-time polymerase chain reaction
PBS	Phosphate buffered saline
ALP	Alkaline phosphatase
OCN	Osteocalcin

References

1. Zimmermann, G.; Moghaddam, A. Allograft bone matrix versus synthetic bone graft substitutes. *Injury* **2011**, *42*, S16–S21. [[CrossRef](#)] [[PubMed](#)]
2. Gómez-Barrena, E.; Rosset, P.; Müller, I.; Giordano, R.; Bunu, C.; Layrolle, P.; Konttinen, Y.T.; Luyten, F.P. Bone regeneration: Stem cell therapies and clinical studies in orthopaedics and traumatology. *J. Cell. Mol. Med.* **2011**, *15*, 1266–1286. [[CrossRef](#)] [[PubMed](#)]
3. Lichte, P.; Pape, H.C.; Pufe, T.; Kobbe, P.; Fischer, H. Scaffolds for bone healing: Concepts, materials and evidence. *Injury* **2011**, *42*, 569–573. [[CrossRef](#)] [[PubMed](#)]
4. Burchardt, H. Biology of bone transplantation. *Orthop. Clin. N. Am.* **1987**, *18*, 187–196.

5. Buser, Z.; Brodke, D.S.; Youssef, J.A.; Meisel, H.-J.; Myhre, S.L.; Hashimoto, R.; Park, J.-B.; Tim Yoon, S.; Wang, J.C. Synthetic bone graft versus autograft or allograft for spinal fusion: A systematic review. *J. Neurosurg. Spine* **2016**, *25*, 509–516. [[CrossRef](#)] [[PubMed](#)]
6. Schmitz, J.P.; Hollinger, J.O. The critical size defect as an experimental model for craniomandibulofacial nonunions. *Clin. Orthop. Relat. Res.* **1986**, *205*, 299–308. [[CrossRef](#)]
7. Khaled, E.G.; Saleh, M.; Hindocha, S.; Griffin, M.; Khan, W.S. Tissue engineering for bone production- stem cells, gene therapy and scaffolds. *Open Orthop. J.* **2011**, *5* (Suppl. 2), 289–295. [[CrossRef](#)] [[PubMed](#)]
8. Derubeis, A.R.; Cancedda, R. Bone marrow stromal cells (BMSCs) in bone engineering: Limitations and recent advances. *Ann. Biomed. Eng.* **2004**, *32*, 160–165. [[CrossRef](#)] [[PubMed](#)]
9. Gneccchi, M.; Melo, L.G. Bone Marrow-Derived Mesenchymal Stem Cells: Isolation, Expansion, Characterization, Viral Transduction, and Production of Conditioned Medium. *Methods Mol. Biol.* **2009**, *482*, 281–294. [[PubMed](#)]
10. McElreavey, K.D.; Irvine, A.I.; Ennis, K.T.; McLean, W.H. Isolation, culture and characterisation of fibroblast-like cells derived from the Wharton’s jelly portion of human umbilical cord. *Biochem. Soc. Trans.* **1991**, *19*, 29S. [[CrossRef](#)] [[PubMed](#)]
11. Gruber, H.E.; Deepe, R.; Hoelscher, G.L.; Ingram, J.A.; Norton, H.J.; Scannell, B.; Loeffler, B.J.; Zinchenko, N.; Hanley, E.N.; Tapp, H. Human adipose-derived mesenchymal stem cells: Direction to a phenotype sharing similarities with the disc, gene expression profiling, and coculture with human annulus cells. *Tissue Eng. Part A* **2010**, *16*, 2843–2860. [[CrossRef](#)] [[PubMed](#)]
12. In ’t Anker, P.S.; Scherjon, S.A.; Kleijburg-van der Keur, C.; de Groot-Swings, G.M.J.S.; Claas, F.H.J.; Fibbe, W.E.; Kanhai, H.H.H. Isolation of Mesenchymal Stem Cells of Fetal or Maternal Origin from Human Placenta. *Stem Cells* **2004**, *22*, 1338–1345. [[CrossRef](#)] [[PubMed](#)]
13. Genova, T.; Munaron, L.; Carossa, S.; Mussano, F. Overcoming physical constraints in bone engineering: ‘the importance of being vascularized’. *J. Biomater. Appl.* **2016**, *30*, 940–951. [[CrossRef](#)] [[PubMed](#)]
14. De Bari, C.; Dell’Accio, F.; Tylzanowski, P.; Luyten, F.P. Multipotent mesenchymal stem cells from adult human synovial membrane. *Arthritis Rheum.* **2001**, *44*, 1928–1942. [[CrossRef](#)]
15. Ponnaiyan, D.; Bhat, K.M.; Bhat, G.S. Comparison of Immuno-Phenotypes of Stem Cells from Human Dental Pulp and Periodontal Ligament. *Int. J. Immunopathol. Pharmacol.* **2012**, *25*, 127–134. [[CrossRef](#)] [[PubMed](#)]
16. Estrela, C.; de Alencar, A.H.G.; Kitten, G.T.; Vencio, E.F.; Gava, E. Mesenchymal stem cells in the dental tissues: Perspectives for tissue regeneration. *Braz. Dent. J.* **2011**, *22*, 91–98. [[CrossRef](#)] [[PubMed](#)]
17. Zuk, P.A.; Zhu, M.; Mizuno, H.; Huang, J.; Futrell, J.W.; Katz, A.J.; Benhaim, P.; Lorenz, H.P.; Hedrick, M.H. Multilineage Cells from Human Adipose Tissue: Implications for Cell-Based Therapies. *Tissue Eng.* **2001**, *7*, 211–228. [[CrossRef](#)] [[PubMed](#)]
18. Bourin, P.; Bunnell, B.A.; Casteilla, L.; Dominici, M.; Katz, A.J.; March, K.L.; Redl, H.; Rubin, J.P.; Yoshimura, K.; Gimble, J.M. Stromal cells from the adipose tissue-derived stromal vascular fraction and culture expanded adipose tissue-derived stromal/stem cells: A joint statement of the International Federation for Adipose Therapeutics and Science (IFATS) and the International Society for Cellular Therapy (ISCT). *Cytotherapy* **2013**, *15*, 641–648. [[CrossRef](#)] [[PubMed](#)]
19. Uzbass, F.; May, I.D.; Parisi, A.M.; Thompson, S.K.; Kaya, A.; Perkins, A.D.; Memili, E. Molecular Physiognomies and Applications of Adipose-Derived Stem Cells. *Stem Cell Rev. Rep.* **2015**, *11*, 298–308. [[CrossRef](#)] [[PubMed](#)]
20. Miura, M.; Gronthos, S.; Zhao, M.; Lu, B.; Fisher, L.W.; Robey, P.G.; Shi, S. SHED: Stem cells from human exfoliated deciduous teeth. *Proc. Natl. Acad. Sci. USA* **2003**, *100*, 5807–5812. [[CrossRef](#)] [[PubMed](#)]
21. De Mendonca Costa, A.; Bueno, D.F.; Martins, M.T.; Kerkis, I.; Kerkis, A.; Fanganiello, R.D.; Cerruti, H.; Alonso, N.; Passos-Bueno, M.R. Reconstruction of large cranial defects in nonimmunosuppressed experimental design with human dental pulp stem cells. *J. Craniofac. Surg.* **2008**, *19*, 204–210. [[CrossRef](#)] [[PubMed](#)]
22. Ma, L.; Makino, Y.; Yamaza, H.; Akiyama, K.; Hoshino, Y.; Song, G.; Kukita, T.; Nonaka, K.; Shi, S.; Yamaza, T. Cryopreserved Dental Pulp Tissues of Exfoliated Deciduous Teeth Is a Feasible Stem Cell Resource for Regenerative Medicine. *PLoS ONE* **2012**, *7*, e51777. [[CrossRef](#)] [[PubMed](#)]
23. Leyendecker Junior, A.; Gomes Pinheiro, C.C.; Lazzaretti Fernandes, T.; Franco Bueno, D. The use of human dental pulp stem cells for in vivo bone tissue engineering: A systematic review. *J. Tissue Eng.* **2018**, *9*, 204173141775276. [[CrossRef](#)] [[PubMed](#)]

24. Yorukoglu, A.C.; Kiter, A.E.; Akkaya, S.; Satiroglu-Tufan, N.L.; Tufan, A.C. A Concise Review on the Use of Mesenchymal Stem Cells in Cell Sheet-Based Tissue Engineering with Special Emphasis on Bone Tissue Regeneration. *Stem Cells Int.* **2017**, *2017*, 1–13. [[CrossRef](#)] [[PubMed](#)]
25. Mussano, F.; Genova, T.; Corsalini, M.; Schierano, G.; Pettini, F.; di Venere, D.; Carossa, S. Cytokine, Chemokine, and Growth Factor Profile Characterization of Undifferentiated and Osteoinduced Human Adipose-Derived Stem Cells. *Stem Cells Int.* **2017**, *2017*, 1–11. [[CrossRef](#)] [[PubMed](#)]
26. Yamaguchi, S.; Shibata, R.; Yamamoto, N.; Nishikawa, M.; Hibi, H.; Tanigawa, T.; Ueda, M.; Murohara, T.; Yamamoto, A. Dental pulp-derived stem cell conditioned medium reduces cardiac injury following ischemia-reperfusion. *Sci. Rep.* **2015**, *5*, 16295. [[CrossRef](#)] [[PubMed](#)]
27. Roato, I.; Alotto, D.; Belisario, D.C.; Casarin, S.; Fumagalli, M.; Cambieri, I.; Piana, R.; Stella, M.; Ferracini, R.; Castagnoli, C. Adipose Derived-Mesenchymal Stem Cells Viability and Differentiating Features for Orthopaedic Reparative Applications: Banking of Adipose Tissue. *Stem Cells Int.* **2016**, *2016*, 1–11. [[CrossRef](#)] [[PubMed](#)]
28. Correia, S.I.; Pereira, H.; Silva-Correia, J.; Van Dijk, C.N.; Espregueira-Mendes, J.; Oliveira, J.M.; Reis, R.L. Current concepts: Tissue engineering and regenerative medicine applications in the ankle joint. *J. R. Soc. Interface* **2014**, *11*, 20130784. [[CrossRef](#)] [[PubMed](#)]
29. Samsonraj, R.M.; Raghunath, M.; Nurcombe, V.; Hui, J.H.; van Wijnen, A.J.; Cool, S.M. Concise Review: Multifaceted Characterization of Human Mesenchymal Stem Cells for Use in Regenerative Medicine. *Stem Cells Transl. Med.* **2017**. [[CrossRef](#)] [[PubMed](#)]
30. Gimble, J.M.; Katz, A.J.; Bunnell, B.A. Adipose-derived stem cells for regenerative medicine. *Circ. Res.* **2007**, *100*, 1249–1260. [[CrossRef](#)] [[PubMed](#)]
31. Lendeckel, S.; Jödicke, A.; Christophis, P.; Heidinger, K.; Wolff, J.; Fraser, J.K.; Hedrick, M.H.; Berthold, L.; Howaldt, H.-P. Autologous stem cells (adipose) and fibrin glue used to treat widespread traumatic calvarial defects: Case report. *J. Cranio-Maxillofac. Surg.* **2004**, *32*, 370–373. [[CrossRef](#)] [[PubMed](#)]
32. Kobolak, J.; Dinnyes, A.; Memic, A.; Khademhosseini, A.; Mobasheri, A. Mesenchymal stem cells: Identification, phenotypic characterization, biological properties and potential for regenerative medicine through biomaterial micro-engineering of their niche. *Methods* **2016**, *99*, 62–68. [[CrossRef](#)] [[PubMed](#)]
33. DuPont, N.C.; Wang, K.; Wadhwa, P.D.; Culhane, J.F.; Nelson, E.L. Validation and comparison of luminex multiplex cytokine analysis kits with ELISA: Determinations of a panel of nine cytokines in clinical sample culture supernatants. *J. Reprod. Immunol.* **2005**, *66*, 175–191. [[CrossRef](#)] [[PubMed](#)]
34. Mussano, F.; Genova, T.; Munaron, L.; Petrillo, S.; Erovigni, F.; Carossa, S. Cytokine, chemokine, and growth factor profile of platelet-rich plasma. *Platelets* **2016**, *27*, 467–471. [[CrossRef](#)] [[PubMed](#)]
35. Nakamura, T.; Nishizawa, T.; Hagiya, M.; Seki, T.; Shimonishi, M.; Sugimura, A.; Tashiro, K.; Shimizu, S. Molecular cloning and expression of human hepatocyte growth factor. *Nature* **1989**, *342*, 440–443. [[CrossRef](#)] [[PubMed](#)]
36. Montesano, R.; Matsumoto, K.; Nakamura, T.; Orci, L. Identification of a fibroblast-derived epithelial morphogen as hepatocyte growth factor. *Cell* **1991**, *67*, 901–908. [[CrossRef](#)]
37. Nakamura, T.; Sakai, K.; Nakamura, T.; Matsumoto, K. Hepatocyte growth factor twenty years on: Much more than a growth factor. *J. Gastroenterol. Hepatol.* **2011**, *26*, 188–202. [[CrossRef](#)] [[PubMed](#)]
38. Lau, T.T.; Wang, D.-A. Stromal cell-derived factor-1 (SDF-1): Homing factor for engineered regenerative medicine. *Expert Opin. Biol. Ther.* **2011**, *11*, 189–197. [[CrossRef](#)] [[PubMed](#)]
39. Hofer, H.R.; Tuan, R.S. Secreted trophic factors of mesenchymal stem cells support neurovascular and musculoskeletal therapies. *Stem Cell Res. Ther.* **2016**, *7*, 131. [[CrossRef](#)] [[PubMed](#)]
40. Dufrane, D. Impact of Age on Human Adipose Stem Cells for Bone Tissue Engineering. *Cell Transplant.* **2017**, *26*, 1496–1504. [[CrossRef](#)] [[PubMed](#)]
41. Siegel, K.R.; Clevenger, T.N.; Clegg, D.O.; Proctor, D.A.; Proctor, C.S. Adipose Stem Cells Incorporated in Fibrin Clot Modulate Expression of Growth Factors. *Arthrosc. J. Arthrosc. Relat. Surg.* **2017**, *34*, 581–591. [[CrossRef](#)] [[PubMed](#)]
42. Murohara, T.; Shintani, S.; Kondo, K. Autologous adipose-derived regenerative cells for therapeutic angiogenesis. *Curr. Pharm. Des.* **2009**, *15*, 2784–2790. [[CrossRef](#)] [[PubMed](#)]
43. Park, B.S.; Jang, K.A.; Sung, J.H.; Park, J.S.; Kwon, Y.H.; Kim, K.J.; Kim, W.S. Adipose-derived stem cells and their secretory factors as a promising therapy for skin aging. *Dermatol. Surg.* **2008**, *34*, 1323–1326. [[CrossRef](#)] [[PubMed](#)]

44. Walsh, K.; Perlman, H. Cell cycle exit upon myogenic differentiation. *Curr. Opin. Genet. Dev.* **1997**, *7*, 597–602. [[CrossRef](#)]
45. Buttitta, L.A.; Edgar, B.A. Mechanisms controlling cell cycle exit upon terminal differentiation. *Curr. Opin. Cell Biol.* **2007**, *19*, 697–704. [[CrossRef](#)] [[PubMed](#)]
46. Waters, R.; Alam, P.; Pacelli, S.; Chakravarti, A.R.; Ahmed, R.P.H.; Paul, A. Stem cell-inspired secretome-rich injectable hydrogel to repair injured cardiac tissue. *Acta Biomater.* **2017**, *69*, 95–106. [[CrossRef](#)] [[PubMed](#)]
47. Denkovskij, J.; Bagdonas, E.; Kusleviciute, I.; Mackiewicz, Z.; Unguryte, A.; Porvaneckas, N.; Fleury, S.; Venalis, A.; Jorgensen, C.; Bernotiene, E. Paracrine Potential of the Human Adipose Tissue-Derived Stem Cells to Modulate Balance between Matrix Metalloproteinases and Their Inhibitors in the Osteoarthritic Cartilage In Vitro. *Stem Cells Int.* **2017**, *2017*, 1–13. [[CrossRef](#)] [[PubMed](#)]
48. Matsushita, Y.; Ishigami, M.; Matsubara, K.; Kondo, M.; Wakayama, H.; Goto, H.; Ueda, M.; Yamamoto, A. Multifaceted therapeutic benefits of factors derived from stem cells from human exfoliated deciduous teeth for acute liver failure in rats. *J. Tissue Eng. Regen. Med.* **2015**, *11*. [[CrossRef](#)] [[PubMed](#)]
49. Wakayama, H.; Hashimoto, N.; Matsushita, Y.; Matsubara, K.; Yamamoto, N.; Hasegawa, Y.; Ueda, M.; Yamamoto, A. Factors secreted from dental pulp stem cells show multifaceted benefits for treating acute lung injury in mice. *Cytotherapy* **2015**, *17*, 1119–1129. [[CrossRef](#)] [[PubMed](#)]
50. Hristov, M.; Zerneck, A.; Liehn, E.A.; Weber, C. Regulation of endothelial progenitor cell homing after arterial injury. *Thromb. Haemost.* **2007**, *98*, 274–277. [[CrossRef](#)] [[PubMed](#)]
51. Koch, A.E.; Polverini, P.J.; Kunkel, S.L.; Harlow, L.A.; DiPietro, L.A.; Elner, V.M.; Elner, S.G.; Strieter, R.M. Interleukin-8 as a macrophage-derived mediator of angiogenesis. *Science* **1992**, *258*, 1798–1801. [[CrossRef](#)] [[PubMed](#)]
52. Mussano, F.; Genova, T.; Verga Falzacappa, E.; Scopece, P.; Munaron, L.; Rivolo, P.; Mandracci, P.; Benedetti, A.; Carossa, S.; Patelli, A. In vitro characterization of two different atmospheric plasma jet chemical functionalizations of titanium surfaces. *Appl. Surf. Sci.* **2017**, *409*, 314–324. [[CrossRef](#)]
53. Mussano, F.; Genova, T.; Rivolo, P.; Mandracci, P.; Munaron, L.; Faga, M.G.; Carossa, S. Role of surface finishing on the in vitro biological properties of a silicon nitride–titanium nitride (Si₃N₄–TiN) composite. *J. Mater. Sci.* **2017**, *52*, 467–477. [[CrossRef](#)]
54. Canullo, L.; Genova, T.; Mandracci, P.; Mussano, F.; Abundo, R.; Fiorellini, J. Morphometric Changes Induced by Cold Argon Plasma Treatment on Osteoblasts Grown on Different Dental Implant Surfaces. *Int. J. Periodontics Restor. Dent.* **2017**, *37*, 541–548. [[CrossRef](#)] [[PubMed](#)]
55. Genova, T.; Grolez, G.P.; Camillo, C.; Bernardini, M.; Bokhobza, A.; Richard, E.; Scianna, M.; Lemonnier, L.; Valdembri, D.; Munaron, L.; et al. TRPM8 inhibits endothelial cell migration via a non-channel function by trapping the small GTPase Rap1. *J. Cell Biol.* **2017**, *216*, 2107–2130. [[CrossRef](#)] [[PubMed](#)]
56. Fiorio Pla, A.; Genova, T.; Pupo, E.; Tomatis, C.; Genazzani, A.; Zaninetti, R.; Munaron, L. Multiple Roles of Protein Kinase A in Arachidonic Acid-Mediated Ca²⁺ Entry and Tumor-Derived Human Endothelial Cell Migration. *Mol. Cancer Res.* **2010**, *8*, 1466–1476. [[CrossRef](#)] [[PubMed](#)]
57. Sacerdote, P.; Mussano, F.; Franchi, S.; Panerai, A.E.; Bussolati, G.; Carossa, S.; Bartorelli, A.; Bussolati, B. Biological components in a standardized derivative of bovine colostrum. *J. Dairy Sci.* **2013**, *96*, 1745–1754. [[CrossRef](#)] [[PubMed](#)]
58. Vallée, A.; Faga, M.G.; Mussano, F.; Catalano, F.; Tolosano, E.; Carossa, S.; Altruda, F.; Martra, G. Alumina-zirconia composites functionalized with laminin-1 and laminin-5 for dentistry: Effect of protein adsorption on cellular response. *Colloids Surf. B Biointerfaces* **2014**, *114*, 284–293. [[CrossRef](#)] [[PubMed](#)]
59. Munaron, L.; Genova, T.; Avanzato, D.; Antoniotti, S.; Fiorio Pla, A. Targeting calcium channels to block tumor vascularization. *Recent Pat. Anticancer Drug Discov.* **2013**, *8*, 27–37. [[CrossRef](#)] [[PubMed](#)]
60. Mussano, F.; Genova, T.; Laurenti, M.; Zicola, E.; Munaron, L.; Rivolo, P.; Mandracci, P.C.S. Early response of fibroblasts and epithelial cells to pink-shaded anodized dental implant abutments: An in vitro study. *Int. J. Oral Maxillofac. Implants* **2018**, in press.
61. Petrillo, S.; Chiabrando, D.; Genova, T.; Fiorito, V.; Ingoglia, G.; Vinchi, F.; Mussano, F.; Carossa, S.; Silengo, L.; Altruda, F.; et al. Heme accumulation in endothelial cells impairs angiogenesis by triggering paraptosis. *Cell Death Differ.* **2017**, *1*. [[CrossRef](#)] [[PubMed](#)]
62. Schierano, G.; Mussano, F.; Faga, M.G.; Menicucci, G.; Manzella, C.; Sabione, C.; Genova, T.; von Degerfeld, M.M.; Peirone, B.; Cassenti, A.; et al. An Alumina Toughened Zirconia Composite for Dental Implant Application: In Vivo Animal Results. *Biomed. Res. Int.* **2015**, *2015*. [[CrossRef](#)] [[PubMed](#)]

63. Roato, I.; Belisario, D.C.; Compagno, M.; Verderio, L.; Sighinolfi, A.; Mussano, F.; Genova, T.; Veneziano, F.; Pertici, G.; Perale, G.; et al. Adipose-derived stromal vascular fraction/xenohybrid bone scaffold: An alternative source for bone regeneration. *Stem Cells Int.* **2018**, *2018*. [[CrossRef](#)]
64. Yang, R.; Davies, C.M.; Archer, C.W.; Richards, R.G. Immunohistochemistry of matrix markers in Technovit 9100 New-embedded undecalcified bone sections. *Eur. Cells Mater.* **2003**, *6*, 57–71. [[CrossRef](#)]
65. Canullo, L.; Genova, T.; Tallarico, M.; Gautier, G.; Mussano, F.; Botticelli, D. Plasma of Argon Affects the Earliest Biological Response of Different Implant Surfaces. *J. Dent. Res.* **2016**, *95*, 566–573. [[CrossRef](#)] [[PubMed](#)]
66. Fiorio Pla, A.; Brossa, A.; Bernardini, M.; Genova, T.; Grolez, G.; Villers, A.; Leroy, X.; Prevarskaya, N.; Gkika, D.; Bussolati, B. Differential sensitivity of prostate tumor derived endothelial cells to sorafenib and sunitinib. *BMC Cancer* **2014**, *14*, 939. [[CrossRef](#)] [[PubMed](#)]



© 2018 by the authors. Licensee MDPI, Basel, Switzerland. This article is an open access article distributed under the terms and conditions of the Creative Commons Attribution (CC BY) license (<http://creativecommons.org/licenses/by/4.0/>).